

Report No. CG-D-07-92

AD-A252 635

2



**EVALUATION OF SEARCH AND RESCUE (SAR) METHOD
FOR DETERMINING LOCAL WIND CURRENT**

J.E. DICK
U.S. Coast Guard
Research and Development Center
1082 Shennecossett Road
Groton, CT 06340-6096

DTIC
S ELECTE D
JUL 10 1992
A

92-18061



INTERIM REPORT
July 1991

This document is available to the U.S. public through the
National Technical Information Service, Springfield, Virginia 22161

This document has been approved
for public release and sale; its
distribution is unlimited.

Prepared for:

U.S. Department Of Transportation
United States Coast Guard
Office of Engineering, Logistics, and Development
Washington, DC 20593-0001

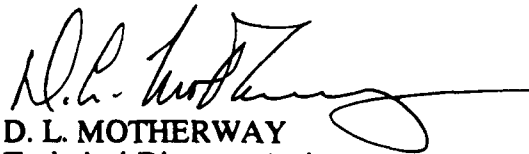
92 7 00 0218

NOTICE

This document is disseminated under the sponsorship of the Department of Transportation in the interest of information exchange. The United States Government assumes no liability for its contents or use thereof.

The United States Government does not endorse products or manufacturers. Trade or manufacturers' names appear herein solely because they are considered essential to the object of this report.

The contents of this report reflect the views of the Coast Guard Research and Development Center, which is responsible for the facts and accuracy of data presented. This report does not constitute a standard, specification, or regulation.



D. L. MOTHERWAY
Technical Director, Acting
United States Coast Guard
Research and Development Center
1082 Shennecossett Road
Groton, CT 06340-6096



Technical Report Documentation Page

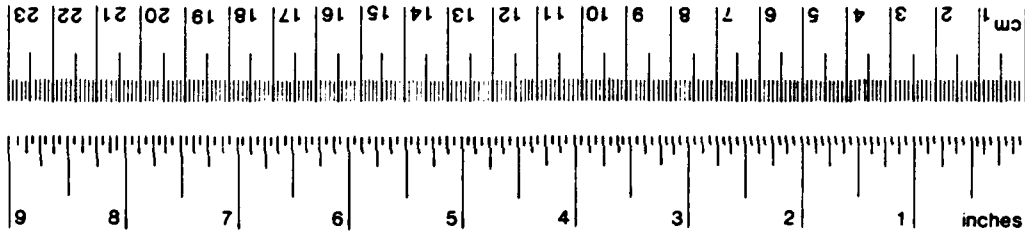
| | | | |
|---|--|--|-----------|
| 1. Report No. CG-D-07-92 | 2. Government Accession No. | 3. Recipient's Catalog No. | |
| 4. Title and Subtitle Evaluation of Search and Rescue (SAR) Method for Determining Local Wind Current | | 5. Report Date July 1991 | |
| | | 6. Performing Organization Code | |
| 7. Author(s) J.E. Dick | | 8. Performing Organization Report No. R&DC 18/91 | |
| 9. Performing Organization Name and Address U.S. Coast Guard Research and Development Center 1082 Shennecossett Road Groton, Connecticut 06340-6096 | | 10. Work Unit No. (TRAVIS) | |
| | | 11. Contract or Grant No. | |
| 12. Sponsoring Agency Name and Address Department of Transportation U.S. Coast Guard Office of Engineering, Logistics, and Development Washington, D.C. 20593-0001 | | 13. Type of Report and Period Covered INTERIM REPORT February - July 1991 | |
| | | 14. Sponsoring Agency Code | |
| 15. Supplementary Notes This report is the fourth in a series that will document the improvement of search and rescue capabilities (ISARC) project at the U.S. Coast Guard R&D Center and thirtieth in a series of R&D reports dealing with search and rescue. | | | |
| 16. Abstract This report discusses a preliminary investigation of the National Search and Rescue (SAR) Manual method for calculating wind driven currents. The SAR Manual recommends a manual method developed by Mooney (1978). The derivation of the model is reviewed and the local wind current predictions are compared with the Mellor-Yamada Level 2 1/2 model (Mellor-Yamada, 1982), a complex one-dimensional model of the mixed layer. Several aspects of the model are assessed for physical correctness. Recommendations for a manual and a numerical method are provided based on the comparison of the predications of the SAR-Mooney model with those of the Mellor-Yamada Level 2 1/2 model. Consequently, these recommendations should be regarded as provisional until the experimental investigation has been performed and the results analyzed. | | | |
| 17. Key Words search and rescue (SAR) wind driven currents Ekman Current | | 18. Distribution Statement Document is available to the U.S. public through the National Technical Information Service, Springfield, Virginia 22161 | |
| 19. Security Classif. (of this report) UNCLASSIFIED | 20. SECURITY CLASSIF. (of this page) UNCLASSIFIED | 21. No. of Pages | 22. Price |

METRIC CONVERSION FACTORS

Approximate Conversions to Metric Measures

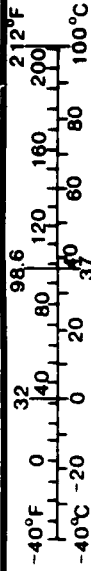
| Symbol | When You Know | Multiply By | To Find | Symbol |
|----------------------------|------------------------|----------------------------|---------------------|-----------------|
| LENGTH | | | | |
| in | inches | * 2.5 | centimeters | cm |
| ft | feet | 30 | centimeters | cm |
| yd | yards | 0.9 | meters | m |
| mi | miles | 1.6 | kilometers | km |
| AREA | | | | |
| in ² | square inches | 6.5 | square centimeters | cm ² |
| ft ² | square feet | 0.09 | square meters | m ² |
| yd ² | square yards | 0.8 | square meters | m ² |
| mi ² | square miles | 2.6 | square kilometers | km ² |
| | acres | 0.4 | hectares | ha |
| MASS (WEIGHT) | | | | |
| oz | ounces | 28 | grams | g |
| lb | pounds | 0.45 | kilograms | kg |
| | short tons (2000 lb) | 0.9 | tonnes | t |
| VOLUME | | | | |
| tsp | teaspoons | 5 | milliliters | ml |
| tbsp | tablespoons | 15 | milliliters | ml |
| fl oz | fluid ounces | 30 | milliliters | ml |
| c | cups | 0.24 | liters | l |
| pt | pints | 0.47 | liters | l |
| qt | quarts | 0.95 | liters | l |
| gal | gallons | 3.8 | liters | l |
| ft ³ | cubic feet | 0.03 | cubic meters | m ³ |
| yd ³ | cubic yards | 0.76 | cubic meters | m ³ |
| TEMPERATURE (EXACT) | | | | |
| °F | Fahrenheit temperature | 5/9 (after subtracting 32) | Celsius temperature | °C |

* 1 in = 2.54 (exactly) For other exact conversions and more detailed tables, see NBS Misc. Publ. 286, Units of Weights and Measures. Price \$2.25. SD Catalog No. C.13.10.286.



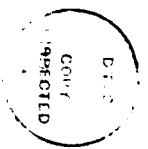
Approximate Conversions from Metric Measures

| Symbol | When You Know | Multiply By | To Find | Symbol |
|----------------------------|-----------------------------------|-------------------|------------------------|-----------------|
| LENGTH | | | | |
| mm | millimeters | 0.04 | inches | in |
| cm | centimeters | 0.4 | inches | in |
| m | meters | 3.3 | feet | ft |
| m | meters | 1.1 | yards | yd |
| km | kilometers | 0.6 | miles | mi |
| AREA | | | | |
| cm ² | square centimeters | 0.16 | square inches | in ² |
| m ² | square meters | 1.2 | square yards | yd ² |
| km ² | square kilometers | 0.4 | square miles | mi ² |
| ha | hectares (10,000 m ²) | 2.5 | acres | |
| MASS (WEIGHT) | | | | |
| g | grams | 0.035 | ounces | oz |
| kg | kilograms | 2.2 | pounds | lb |
| t | tonnes (1000 kg) | 1.1 | short tons | |
| VOLUME | | | | |
| ml | milliliters | 0.03 | fluid ounces | fl oz |
| l | liters | 0.125 | cups | c |
| l | liters | 2.1 | pints | pt |
| l | liters | 1.06 | quarts | qt |
| l | liters | 0.26 | gallons | gal |
| m ³ | cubic meters | 35 | cubic feet | ft ³ |
| m ³ | cubic meters | 1.3 | cubic yards | yd ³ |
| TEMPERATURE (EXACT) | | | | |
| °C | Celsius temperature | 9/5 (then add 32) | Fahrenheit temperature | °F |



Contents

| | |
|---|------|
| List of Figures | vi |
| List of Tables | vii |
| Executive Summary | viii |
| Acknowledgements | x |
| 1 Introduction | 1 |
| 2 Background | 1 |
| 3 The SAR Manual Method | 3 |
| 3.1 Assumptions | 4 |
| 3.1.1 Form of the Wind Stress | 4 |
| 3.1.2 Effect of Tuning Parameters | 6 |
| 3.2 Additional Considerations | 13 |
| 3.2.1 Drift near the equator | 13 |
| 3.2.2 Validity of model in nearshore region | 13 |
| 3.3 Summary | 15 |
| 3.3.1 Form of the wind stress | 15 |
| 3.3.2 Tuning parameters | 15 |
| 4 Verification by Field Measurements | 16 |
| 5 Recommendations | 17 |
| 5.1 Manual Method | 17 |
| 5.2 Numerical Model | 18 |
| 6 References | 19 |
| A Appendix | A-1 |



| | |
|--------------------|-------------------------------------|
| Accession For | |
| NTIS CRA&I | <input checked="" type="checkbox"/> |
| DTIC TAB | <input type="checkbox"/> |
| Unannounced | <input type="checkbox"/> |
| Justification | |
| By | |
| Distribution/ | |
| Availability Codes | |
| Dist | Avail and/or Special |
| A-1 | |

List of Figures

- 1 Ekman depth as a function of wind speed and latitude. 9
- 2 Variation of inertial period with latitude. 11
- 3 A progressive vector diagram for a particle when a westerly wind suddenly rises at time $t = 0$ and later changes to the northwest. 12

List of Tables

- 1 Comparison of wind current and direction for Mellor-Yamada model with SAR-Mooney model at 45° N, depth is 0.6 m. . . . 5
- 2 Comparison of wind current and direction for Mellor-Yamada model with SAR-Mooney model at 45° N, depth is 6.9 m. . . . 7
- 3 Comparison of wind current and direction for Mellor-Yamada model with SAR-Mooney model for a range of latitudes. . . . 13

Executive Summary

The National Search and Rescue (SAR) Manual describes a method for calculating wind driven currents which is based on a manual method developed by Mooney (1978). This report discusses a preliminary investigation of the model to determine its usefulness in search and rescue applications. The derivation of the model has been reviewed to verify that it is physically correct. It has been compared with the Mellor-Yamada Level $2\frac{1}{2}$ model (Mellor and Yamada, 1982), a complex one dimensional model of the mixed layer. Several aspects of the model have been assessed and the conclusions will be summarized below.

In comparison with the Mellor-Yamada Level $2\frac{1}{2}$ model, the SAR-Mooney model over-estimated the deviation of the current direction from the wind direction for the entire range of wind velocities examined (2.5 to 40 m/s [5 to 80 knots]). The model predictions of current velocity agreed well with a steady wind speed of 10 m/s (20 knots), but the difference between the models increased with increasing windspeed.

The SAR-Mooney model was tuned with subsurface current data from 12 m, however, when compared with the Mellor-Yamada model, it agreed with near-surface predictions. Although this result suggests that the SAR-Mooney model may not describe well the experimental data on which its coefficients are based, it does not appear to be a drawback to its use.

Mooney (1978) determined his model's coefficients with data from relatively deep water compared with the depth limitation recommended by the National SAR Manual of 30 m (100 feet). Where the water depth is equal to or greater than the Ekman depth which is the depth of the bottom layer influenced by the wind stress, the wind drift should not be affected by the water depth. At depths shallower than the Ekman depth, the SAR-Mooney predictions should be treated with caution. Figure 1 may be used to estimate the limiting depth for which the water can be assumed to be infinitely deep as a function of windspeed and latitude.

Mooney (1978) tuned his model with wind and current data from about 39° N. It appears that the SAR-Mooney model may be increasingly inaccurate as the equator is approached, particularly with respect to the magnitude of the current.

In the vicinity of the equator, the inertial frequency approaches zero, so the wind drift is dependent only on the wind stress and therefore, the drift

will be in the direction of the wind.

The recommended limitation of the SAR-Mooney method to cases greater than 32 km (20 miles) from the coast appears to be too short a distance. Wind drift will be affected by a coastal barrier at a distance equal to or less than the Rossby radius. As the water depth decreases, the effect of the coastline increases. Additionally, the effect of the coast increases linearly with decreasing distance from the coast.

Acknowledgements

Dr. G.L. Mellor of Princeton University graciously provided the computer code of his model to Dr. J. O'Donnell of the University of Connecticut, Avery Point, who allowed access to his computing facilities and contributed many helpful suggestions.

1 Introduction

A quantitative understanding of the mechanics of wind generated currents is of great importance to oceanographers and others concerned with such practical problems as search and rescue, oil spill propagation and iceberg drift. These types of problems have a need for near real-time estimates of the local wind driven current. The National Search and Rescue (SAR) Manual describes a technique for calculating the local wind current which is based on a manual method developed by Mooney (1978). This method has also been incorporated into Computer Assisted Search Planning (CASP) and the iceberg drift model used by the International Ice Patrol (IIP).

The purpose of this report is to examine the National SAR Manual method for determining local wind driven current and to address the following questions: (1) is the SAR method physically correct; (2) does the SAR method accurately describe the wind generated currents; (3) is this method sufficient for the needs of SAR; (4) is this method acceptable for the IIP to predict iceberg motion; or, (5) does it need to be corrected or replaced by another model for determining wind current? An experimental investigation is planned that is designed to compare the predictions of the SAR-Mooney model with field measurements. The results will be presented in a subsequent report.

2 Background

Before the merits of the model can be discussed, it is necessary to understand the mechanisms by which wind generates local current. When wind blows over the earth's surface, a stress is exerted on the surface, whether this be solid ground or sea. This stress is a considerable retarding force on the atmosphere and a driving force for the ocean. The wind stress produces a direct response called the Ekman component of the current. This current is mainly confined to a thin layer (on the order of 10 to 100 m deep) near the ocean surface, usually within the upper mixed layer (Gill, 1982). Pure drift currents are generated by the drag of the wind passing over homogenous water. At first, the resulting current follows the direction of the wind, but as a consequence of the earth's rotation, the Coriolis effect causes the current to deviate from the wind direction. As each water layer moves, it exerts a

stress on the layer beneath it, so that each layer deviates even more from the wind direction than the layer above it.

Ekman (1905) was the first to examine the oceanic response to time-dependent wind forcing. By assuming an infinitely deep ocean (to neglect bottom friction), unbounded in the horizontal direction, with a steady wind blowing over a homogenous ocean with a level sea surface (so the pressure gradient is zero), the magnitude and direction of the Ekman velocity can be found as a balance between the local accelerations and the Coriolis force with the vertical gradient of the horizontal stress. Thus, the linearized equation can be written:

$$\frac{\partial w}{\partial t} + ifw = \nu \frac{\partial^2 w}{\partial z^2} \quad (1)$$

where $w = u + iv$, the complex current, of which u is eastward velocity and v is northward velocity, $f = 2\Omega \sin \phi$ is the Coriolis parameter, (Ω is the earth's angular velocity and ϕ is the latitude), ν is the kinematic eddy viscosity, and z is the vertical coordinate, positive upward. Only vertical derivatives of horizontal stresses are included in Equation 1 because the vertical scale of oceanic boundary layers is much smaller than the horizontal scale over which the stresses vary (Gill, 1982).

Ekman assumed that the kinematic eddy viscosity was constant with depth to simplify the equations and also because little was known about the variation of the eddy viscosity with depth. If we assume that the sea is initially at rest, and that the wind rises suddenly and is maintained at a constant speed, then the solution to Equation 1, assuming a constant eddy viscosity, is given by

$$w = -\frac{i\nu}{f} (1 - e^{-ift}) \frac{\partial^2 w}{\partial z^2}. \quad (2)$$

Jelesnianski (1970) obtained a solution to Equation 1 for the more complicated problem of an arbitrary time-dependent wind:

$$w(z, t) = \frac{2}{H} \sum_{n=0}^{\infty} \cos \left[\left(n + \frac{1}{2} \right) \pi \frac{z}{H} \right] \int_0^t F(t - \tau) e^{-\theta_n \tau} dt \quad (3)$$

where H is the water depth, and

$$\theta_n = if + \left[n + \frac{1}{2} \right]^2 \frac{\nu \pi^2}{H^2} \quad (4)$$

with the boundary conditions,

$$w(-H, t) = 0, \quad w(z, 0) = \left. \frac{\partial w}{\partial t} \right|_{t=0} = 0, \quad \nu \left. \frac{\partial w}{\partial z} \right|_{z=0} = F(t) \quad (5)$$

where $F(t)$ is the wind stress. The derivation of equation 3 can be found in Appendix 1.

Equation 3 forms the basis to the manual method of solution derived by Mooney (1978).

3 The SAR Manual Method

Jelesnianski (1970) based his model on the assumptions made by Ekman (1905), which are listed below:

1. no horizontal boundaries (neglect boundary effects);
2. infinitely deep water (to avoid bottom friction);
3. constant kinematic eddy viscosity (for simplification and also because little was known about the variation of the eddy viscosity with depth);
4. steady wind blowing for a long time (steady-state conditions);
5. homogeneous water and level sea surface (hydrostatic pressure);
6. constant Coriolis parameter.

Although these assumptions are too restrictive for problems with large areal extent where the variation in the Coriolis parameter, density stratification, and lateral stresses are too important to be neglected, Ekman's theory may be sufficient for problems of limited area where the lateral variation in stress is much smaller than the vertical variations (Jelesnianski, 1970). Verification of Ekman's theory is difficult because pure drift currents that satisfy the assumptions above are rarely found in nature and because the vertical distribution of the eddy viscosity is poorly understood, thus precluding a direct comparison of the theory with field measurements. However, it has been observed that simple models describe well measurements of velocity fluctuations in the mixed layer (Gill, 1982).

3.1 Assumptions

In addition to Ekman's simplifying assumptions, Mooney (1978) made several other assumptions in deriving and tuning his model. The validity of these assumptions and their effects on the calculated wind drift current were examined by comparison of Mooney's method with the one-dimensional version of the mixed layer model developed by Mellor and Yamada (1982). A comparison of the Mellor-Yamada Level $2\frac{1}{2}$ model with other commonly used oceanic mixed-layer models (namely, Mellor-Yamada Level 2, Niiler, Garwood, Price, and Therry-Lacarrere) can be found in Martin (1986). Comparisons were made for cases with both idealized forcing and data from three field experiments. Noticeable discrepancies among the models were observed. In particular, significant differences were discovered for the increase in the depth of the mixed layer in autumn and winter due to wind mixing and convection, and for the decrease in depth of the mixed layer during light winds and strong heating. The Mellor-Yamada Level $2\frac{1}{2}$ model was found to underpredict the mixed-layer depth when compared with field measurements. Additionally, the predicted mixed layer was not as well mixed as indicated by the measurements. However, the model did predict well the smooth gradient at the base of the mixed layer (Martin, 1986).

3.1.1 Form of the Wind Stress

To solve Equation 3, the form of the wind stress must be known or predicted. The wind stress is usually expressed in terms of a drag coefficient and the wind speed. The value of the drag coefficient depends on the roughness of the underlying surface. For winds over water, the roughness of the water surface can vary with wind speed (i.e., surface waves). Therefore, the drag coefficient should not be considered a constant, but rather dependent on wave speed. Owing to the difficulties in wind stress estimates, many oceanographers use the quadratic law, first applied by Ekman,

$$F(t) = \rho_a C_D W^2 \quad (6)$$

where ρ_a is the density of air and the drag coefficient, C_D , is assumed equal to 2.6×10^{-3} , and $W = W_x + iW_y$, is the complex wind velocity, W_x and W_y represent the westerly and southerly wind velocities, respectively. Mooney

| Wind Speed m/s | Mellor-Yamada | | SAR-Mooney | | d km |
|-------------------|----------------|-----------|----------------|-----------|---------|
| | Current m/s | Direction | Current m/s | Direction | |
| 2.5 | 0.03 | 40 | 0.04 | 48 | 0.35 |
| 5.0 | 0.07 | 40 | 0.08 | 48 | 0.44 |
| 10.0 | 0.16 | 30 | 0.15 | 48 | 1.11 |
| 20.0 | 0.37 | 27 | 0.30 | 48 | 3.11 |
| 40.0 | 0.82 | 25 | 0.60 | 48 | 8.04 |

Table 1: Comparison of wind current and direction for Mellor-Yamada model with SAR-Mooney model at 45° N. Water depth is 250 m. Winds from the south at constant velocity for 48 hours. Mellor-Yamada current predictions at depth 0.6 m. The difference over six hours in the model predictions, d , is given by Equation 8.

assumed that the wind stress was linearly proportional to the wind velocity

$$F(t) = \rho_a C_D W(t) \quad (7)$$

and that the wind drag coefficient, $C_D = 1.9 \times 10^{-3}$ cm/sec.

Stress is expressed dimensionally as mass/length/time². So although the drag coefficient is usually taken to be dimensionless Mooney had to assume a dimensional drag coefficient to make his expression dimensionally correct. To simplify the computations, Mooney assumed a linear relation between wind speed and stress, which may restrict the method's applicability to a limited range of wind velocities. Unfortunately, Mooney (1978) does not provide any statistical information on the wind data used to tune his model, so the range of wind velocities over which this method should be most accurate is not known. Therefore, the wind drift calculated from Mooney's model were compared with the predictions from the Mellor-Yamada model for a range of wind velocities. Table 1 lists the results for both models for a constant, southerly wind at 45° N.

Within the range of wind speeds examined, the SAR-Mooney model over-predicted the amount of rotation of the current from the wind direction. At low wind velocities (< 10 m/s [20 knots]), this was not significant, however,

the difference between the current directions predicted by the two models increases with increasing wind velocity. There is a large jump in the disagreement between the models as the wind increases from 5 to 10 m/s (10 to 20 knots), and then a leveling off with increasing wind speed. The percent error is greatest at the lowest wind speeds. However, at low currents the distance drifted is less, so the difference between the spatial drift over time predicted by the models is much lower than at high wind speeds. The difference in the distance drifted over six hours can be calculated from the solution for oblique triangles:

$$d = 6 \left[w_M^2 + w_{MY}^2 - 2w_M w_{MY} \cos(\phi_M - \phi_{MY}) \right]^{1/2} \quad (8)$$

where the subscripts M and MY denote the SAR-Mooney and Mellor-Yamada predictions, respectively. At 10 m/s (20 knots), the SAR-Mooney model changes from overpredicting the current to underpredicting it for higher velocity winds. However, before drawing conclusions based on these results it should be understood that only one wind direction and latitude was examined.

3.1.2 Effect of Tuning Parameters

The validity of Mooney's model may be limited somewhat by the parameters he used to tune his model. Mooney used subsurface current measurements ($H = -12$ m) from approximately 39° N, in water of depth 2682 m. Without justification, Mooney assumed that 48 hours of wind speed and direction data would be sufficient to estimate the wind generated current. Using the Mellor-Yamada model for comparison, the effect of tuning the model with the assumed parameters are considered below. These parameters include (1) the subsurface current record; (2) the water depth; (3) the length of the wind and current record; and (4) variations in latitude, in particular wind drift predictions at the equator.

Subsurface current record Mooney (1978) tuned his model with a time series of current measurements recorded at a depth of 12 m. Since the effects of the Ekman velocity are dissipated with depth, it is reasonable to suspect that the model would underpredict the magnitude and rotation of the surface current. However, when compared with the Mellor-Yamada model, the

| Wind Speed m/s | Mellor-Yamada | | SAR-Mooney | | d km |
|-------------------|----------------|-----------|----------------|-----------|---------|
| | Current m/s | Direction | Current m/s | Direction | |
| 2.5 | 0.01 | 76 | 0.04 | 48 | 0.70 |
| 5.0 | 0.03 | 76 | 0.08 | 48 | 1.20 |
| 10.0 | 0.08 | 59 | 0.15 | 48 | 1.72 |
| 20.0 | 0.20 | 49 | 0.30 | 48 | 2.33 |
| 40.0 | 0.47 | 43 | 0.60 | 48 | 3.07 |

Table 2: Comparison of wind current and direction for Mellor-Yamada model with SAR-Mooney model at 45° N. Water depth is 250 m. Winds from the south at constant velocity for 48 hours. Mellor-Yamada current predictions at depth 6.9 m. The difference over six hours in the model predictions, d , is given by Equation 8.

Mooney model predictions were inconsistent. Table 2 lists the currents at a depth of 6.9 m predicted by the Mellor-Yamada model. For wind speeds under 20 m/s (40 knots), Mooney's model underpredicted the rotation of the current in comparison with Mellor's model and for the range of wind velocities examined, Mooney's model overpredicted the magnitude of the current. Mooney's predictions were in better agreement with Mellor's near the surface (see Table 1) than near the depth of his current data which he used to determine the coefficients. For wind drift calculations, we are not particularly interested in the currents except in the vicinity of the surface, however, it should be noted that the observed better agreement near the surface of the predictions is serendipitous.

Water depth The SAR manual states that wind current should be determined for water depths greater than 30 m (100 ft). Since the coefficients for Mooney's model were calculated in much deeper water and one of the assumptions in Ekman's theory is that the water is infinitely deep, it is relevant to ascertain if this model is valid in shallower water. Ekman assumed an infinitely deep ocean so the surface and the bottom frictional layers (known as the Ekman layers) would not meet. Where the water depth is on the

order of the Ekman depth or less, the surface and bottom layer meet and can even overlap. The two spirals tend to cancel each other with the result that the total transport is more in the direction of the surface wind. When the water depth decreases to about one tenth of the Ekman depth, the transport is essentially in the direction of the wind because the Coriolis effect is overpowered by frictional effects (Pond and Pickard, 1983).

The Ekman depth,

$$D = \pi \sqrt{2\nu/\rho f} \quad (9)$$

where ρ is the density of sea water, is independent of the wind stress, however, it does increase with increasing eddy viscosity and with decreasing latitude. At the equator, the Ekman depth approaches infinity. Therefore, the water depth will become increasingly more important as the equator is approached.

As the wind speed increases, the eddy viscosity increases, so the Ekman depth increases. Therefore at high wind speeds and approaching the equator, 30 m is insufficient for the Ekman spiral to develop. An absolute limit for the applicability of the model is not practical due to the complex relationship between wind speed, latitude, water depth and the Ekman depth. Figure 1 shows a plot that can be used to estimate the water depth limit for which the model is valid. Use of the SAR model in water depths shallower than shown in Figure 1 may lead to incorrect estimates of drift velocity and direction.

When the ratio, H/D , between the water depth, H , and the Ekman depth, D , is small, the angle between the wind and the current direction, known as the deflection angle, γ , is small, and the surface current flows nearly in the direction of the wind. As H/D increases, γ is alternately smaller and larger than 45° . When the oceanic depth is approximately equal to the Ekman depth, the assumption of infinitely deep water is reasonable (Neumann and Pierson, 1966). The following table from Neumann and Pierson shows deflection angles for different depth ratios:

| | | | | |
|----------|------|-----|------|------|
| H/D | 0.25 | 0.5 | 0.75 | 1.00 |
| γ | 21.5 | 45 | 45.5 | 45 |

Length of wind and current record The SAR-Mooney method uses a wind data interval of 6 hours for practical rather than physical reasons;

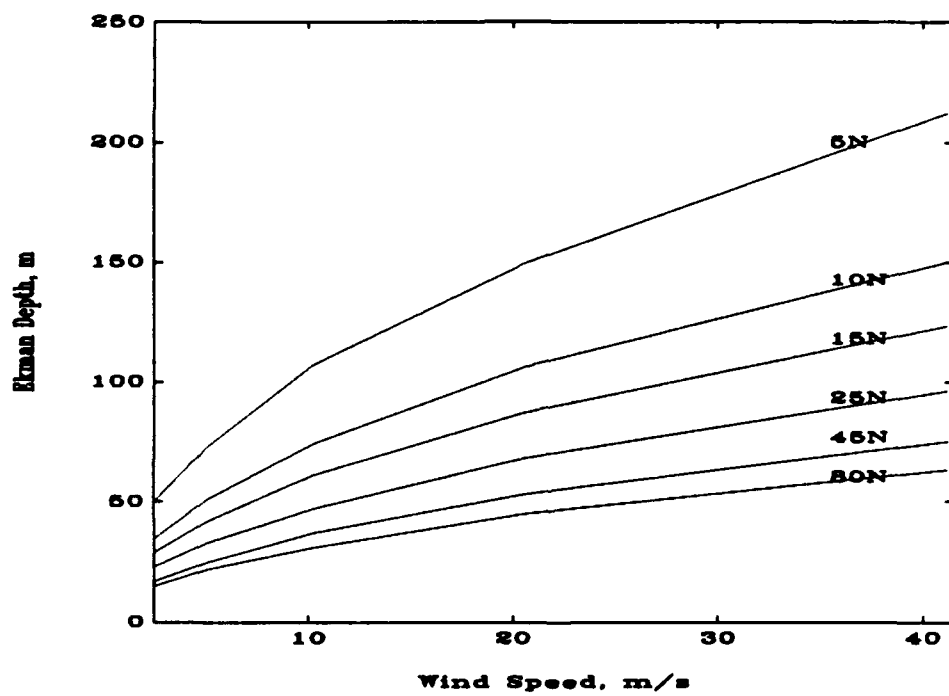


Figure 1: Ekman depth as a function of wind speed and latitude.

the synoptic weather charts are for six hour periods. Without explanation, Mooney used a time record length of 48 hours, which, divided by 6-hour intervals, results in eight time periods. The use of a 48 hour record length without justification is a matter of concern.

Ekman's theory assumes an ocean initially at rest; however, this is rarely found in nature. Inertial oscillations in the ocean often grow to large amplitude and then decay slowly, therefore, the length of the wind record must be long enough for wind generated currents developed by pre-existing wind conditions to have sufficient time to decay. Studies indicate a decay time of several inertial periods (Gill, 1982) where the inertial period is

$$T_i = 2\pi/f. \quad (10)$$

Figures 2a and b show the inertial period as a function of latitude. Since inertial oscillations decay more slowly as the equator is approached, the possibility of the current estimates being incorrect due to the presence of pre-existing inertial oscillations increases.

A sudden change in wind can also reduce or even eliminate pre-existing oscillations. Assume inertial oscillations are present when the wind changes at time $t = t_0$, and w_0 is the value of the Ekman current at time $t = t_0$, then the total Ekman current is,

$$w = \frac{-i\nu}{f} \frac{\partial^2 w}{\partial z^2} + \left\{ w_0 + \frac{i\nu}{f} \frac{\partial^2 w}{\partial z^2} \right\} e^{-if(t-t_0)} \quad (11)$$

where the amplitude of the inertial oscillations is given by the factor in curly brackets. If the wind change occurs at a phase of the pre-existing oscillations when this factor is small, the resulting oscillations will be weak. If the wind change occurs when this factor is large, strong oscillations will occur (Gill, 1982). The effect of the time of the wind change on the amplitude of the inertial oscillations is shown in Figure 3.

It may not be feasible in all cases (particularly in the equatorial region) to go back sufficiently far in the wind record to allow for the decay of any pre-existing inertial oscillations. But for cases where a strong storm has passed recently through the region, the possibility of pre-existing currents should be considered.

Variations in latitude Table 3 compares the predictions of the Mellor-Yamada model with those of the SAR-Mooney model for several latitudes.

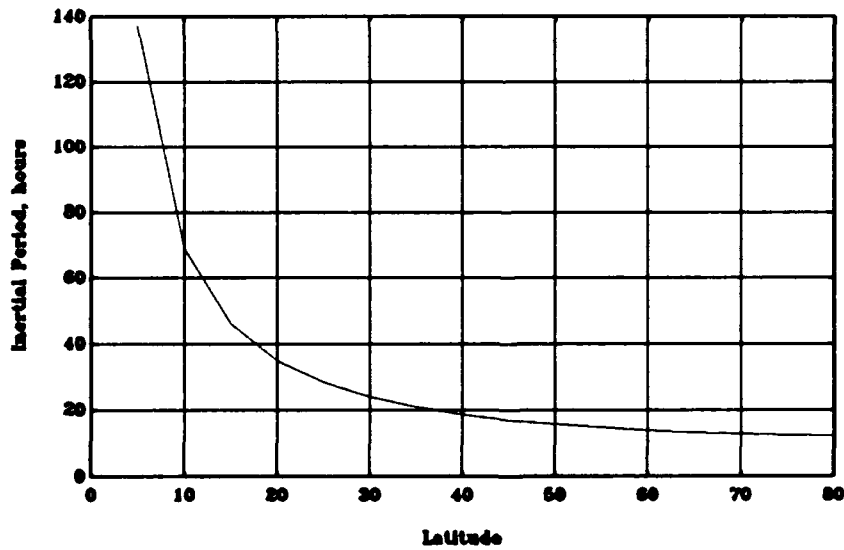
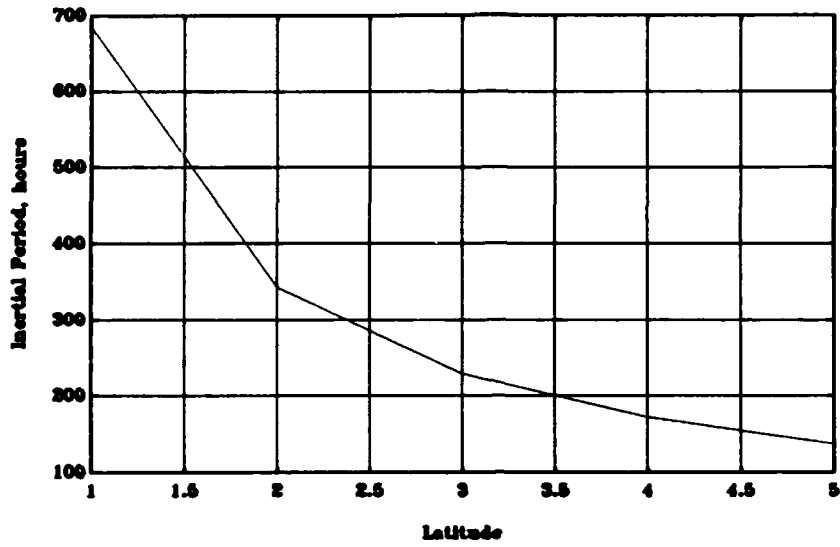


Figure 2: Variation of inertial period with latitude; (a) latitude 1° to 5°, (b) latitude 5° to 80°.

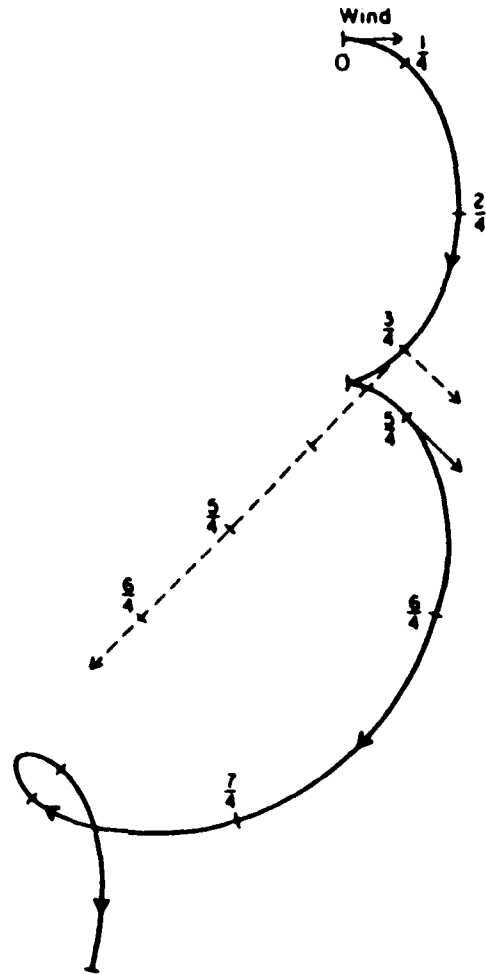


Figure 3: A progressive vector diagram for a particle when a westerly wind suddenly rises at time $t = 0$. Later, the wind changes to the northwest and the wind stress doubles. The solid line depicts the result when the change occurs at $5/4$ inertial periods after $t = 0$. The dashed line shows the result if instead, the wind change occurs at $3/4$ of an inertial period after $t = 0$ (redrawn from Gill, 1982). For further discussion, see Gill, (1982).

| Latitude ° N | Mellor-Yamada | | SAR-Mooney | | d km |
|-----------------|----------------|-----------|----------------|-----------|---------|
| | Current m/s | Direction | Current m/s | Direction | |
| 5 | 0.35 | 29 | 0.68 | 40 | 7.30 |
| 45 | 0.08 | 59 | 0.15 | 48 | 1.72 |
| 65 | 0.16 | 35 | 0.15 | 54 | 1.13 |

Table 3: Comparison of wind current and direction for Mellor-Yamada model with SAR-Mooney model for a range of latitudes. Water depth is 250 m. Winds from the south at 10 m/s (20 knots) for 48 hours. Mellor-Yamada current predictions at depth -6.9 m.

The difference between the two models is much greater in the vicinity of the equator. At 65° N, the agreement is close for the current speed, but less good for the current direction. Further south at 45° N, the agreement of the current speeds is less good than at 65° N, but the directions are in better agreement, and near the equator, at 5° N, the agreement between the velocities is even worse, though the difference between the predicted directions has only increased slightly. This seems to indicate that the errors incurred using the SAR-Mooney model increase as the equator is approached.

3.2 Additional Considerations

3.2.1 Drift near the equator

In the vicinity of the equator, the inertial frequency goes to zero ($f = 2\Omega \sin \phi = 0$) so that the wind drift is dependent solely on the wind stress, and therefore, the drift will essentially be in the direction of the wind.

3.2.2 Validity of model in nearshore region

The SAR manual requires the wind current to be calculated when the distance from shore is greater than 32 km (20 miles). This is based on the effect of a coastal boundary on the development of wind generated currents. Ekman assumed an infinite ocean so that the effects of boundaries could be neglected.

In the vicinity of a barrier, such as a coastline, a convergence or divergence of the Ekman flow occurs, resulting in a piling up of water or in a reduction of the sea level, depending on how the wind is directed with respect to the coastline. In shallow water, flow toward the coast causes water to pile up at the shoreline. Conversely, an offshore flow will cause the sea surface to be lowered near the coast. Therefore, the wind direction with respect to the coastline is important, except where the water depth is considerably smaller than twice the Ekman depth. In this case, the Coriolis effect is negligible (Neumann and Pierson, 1966).

The presence of the shoreline will effect the magnitude and direction of a wind generated current where the distance to the coast is of order of the Rossby radius:

$$a = (gH)^{1/2}/|f|. \quad (12)$$

Thus, in 30 m of water (the SAR Manual recommended depth limit for using the SAR-Mooney model) at 45° N, the Rossby radius is about 160 km (100 miles). Within a Rossby radius of the shoreline, a longshore wind will generate a current towards/away from the coast. Since there can be no flow across the coastline, this steady current will cause a rise/fall in the sea level at the coast in order to conserve mass. Therefore, the sea level and the longshore current will change continually with time (Gill, 1982).

Additionally, wind drift will only be affected by the presence of the coastline when the wind duration is sufficiently long for a surface gravity wave to travel from the shoreline to the point of interest. The time necessary can be calculated from

$$t = L/(gH)^{1/2} \quad (13)$$

where L is the distance to the shore.

Changes in the wind field can affect the Ekman transport in a similar manner as a coastal boundary. For instance, consider the North Pacific or North Atlantic around 25° N between the prevailing westerlies and the Northern Trade Winds. At the boundary between the wind directions, the Ekman transport convergences because both winds transport the water to the right of the wind. This also occurs in the Southern Hemisphere with a transport to the left (Neumann and Pierson, 1966).

3.3 Summary

The National SAR Manual method for calculating wind driven currents has been studied to determine its usefulness in search and rescue applications. The derivations of the model have been reviewed to verify that it is physically correct. It has been compared with one of the most complex one dimensional models of the mixed layer currently available in the literature. Several aspects of the model have been assessed and the conclusions are summarized below.

3.3.1 Form of the wind stress

In comparison with the Mellor-Yamada model, the SAR-Mooney model over-estimated the deviation of the current direction from the wind direction for the entire range of wind velocities examined (2.5 to 40 m/s [5 to 80 knots]). The model predictions of current velocity agreed well with a steady wind speed of 10 m/s (20 knots), but the difference between the models increased with increasing windspeed.

3.3.2 Tuning parameters

Subsurface current record The SAR-Mooney model was tuned with subsurface current data from 12 m, however, when compared with the Mellor-Yamada model, it agreed with near-surface predictions. Although this result suggests that the SAR-Mooney model may not describe well the experimental data on which its coefficients are based, it does not appear to be a drawback to its use.

Water depth Ekman's theory assumes infinitely deep water and Mooney (1978) used data from relatively deep water compared with the depth limitation recommended by the National SAR Manual of 30 m (100 feet). Where the water depth is equal to or greater than the Ekman depth, given by Equation 9, the wind drift should not be affected by the water depth. At depths shallower than the Ekman depth, the SAR-Mooney predictions should be treated with caution. Figure 1 may be used to estimate the limiting depth for which the water can be assumed to be infinitely deep as a function of windspeed and latitude.

Variations in latitude Mooney (1978) tuned his model with wind and current data from about 39° N. It appears that the SAR-Mooney model may be increasingly inaccurate as the equator is approached, particularly with respect to the magnitude of the current.

Equatorial region In the vicinity of the equator, the inertial frequency approaches zero, so the wind drift is dependent only on the wind stress and Equation 1 reduces to

$$\frac{\partial w}{\partial t} = \nu \frac{\partial^2 w}{\partial z^2} \quad (14)$$

so the drift will be in the direction of the wind.

Nearshore region The recommended limitation of the SAR-Mooney method to cases greater than 32 km (20 miles) from the coast appears to be too short a distance. Wind drift will be affected by a coastal barrier at a distance equal to or less than the Rossby radius, (Equation 12). As the water depth decreases, the effect of the coastline increases. Additionally, the effect of the coast increases linearly with decreasing distance from the coast.

4 Verification by Field Measurements

The investigation described in this report was limited to the comparison of two models of wind generated current; one was a complicated one dimensional mixed-layer model while the other was a simple model dependent on carefully determined coefficients. It is useful to compare these models not just against each other, but also with experimental data. An experiment is planned, designed to test the accuracy of the SAR-Mooney model. The measurements obtained from the experiment will be presented in a future report with the results of the model. The comparison of the measurements and model predictions will be used to ascertain the usefulness and limitations of the model for SAR applications.

5 Recommendations

The following recommendations are based on the comparison of the predictions of the SAR-Mooney model with those of the Mellor-Yamada Level $2\frac{1}{2}$ model. Consequently, these recommendations should be regarded as provisional until the experimental investigation has been performed and the results analyzed.

5.1 Manual Method

During this interim period, the SAR-Mooney model should continue to be used for search and rescue and iceberg drift applications with the following caveats:

1. The SAR model over-estimates the deviation of the current from the wind direction.
2. At high wind speeds (over 10 m/s [20 knots]), the SAR model over-estimates the current speed.
3. At depths shallower than the Ekman depth, the results should be treated with caution. Figure 1 may be used to estimate the limiting depth for which the water can be assumed to be infinitely deep as a function of windspeed and latitude.
4. Although at mid and high latitudes, the model predicts well the current speed, the SAR-Mooney model may be increasingly inaccurate as the equator is approached, particularly with respect to the magnitude of the current.
5. In the vicinity of the equator, the drift will be in the direction of the wind.
6. The recommended limitation of the SAR-Mooney method to cases greater than 32 km (20 miles) from the coast appears to be too short a distance. Wind drift will be affected by a coastal barrier at a distance equal to or less than the Rossby radius, $a = (gH)^{1/2}/|f|$.
7. As the water depth decreases, the effect of the coastline increases. Additionally, the effect of the coast increases linearly with decreasing distance from the coast.

5.2 Numerical Model

The SAR-Mooney model should be replaced in CASP by a more complex one dimensional mixed layer model. Several models are discussed in the literature. These models differ in terms of their formulation, complexity, and efficiency (Martin, 1986). The models can generally be described as differential or bulk models, depending on their method of formulation. The differential models use the equations for the conservation of momentum, heat, salt, and turbulent kinetic energy in their primitive form and are not integrated over the mixed layer. The bulk models assume that the mixed layer is well-defined and the equations of conservation are integrated over the mixed layer (Martin, 1986). The most appropriate model for incorporation into CASP will depend on the model formulation and computation ease.

6 References

- Ekman, V.W.** (1905). On the influence of the earth's rotation on ocean currents. *Arch. Mat. Astren. Fys.*, 2(11): 1-53.
- Gill, A.E.** (1982). *Atmosphere - Ocean Dynamics*, Academic Press, 662 pp.
- Jelesnianski, C.P.** (1970). Bottom stress time history in linearized equations of motion for storm surges. *Mon. Weath. Rev.*, Vol 98, pp 462-478.
- Martin, P.J.** (1986). Testing and comparison of several mixed-layer models. *Naval Ocean R & D Activity*, Rep. 143, 30 pp.
- Mellor, G.L. and T. Yamada.** (1982). Development of a turbulence closure model for geophysical fluid problems, *Rev. Geophys. Space Physics*, 20, pp. 851-875.
- Mooney, K.A.** (1978). A method for manually calculating the local wind current. *U.S. Coast Guard, Oceanographic Unit Technical Report 78-2*, 17 pp.
- National SAR Manual** (1986). Vol. I: National Search and Rescue System, U.S. Coast Guard.
- Neumann, G. and W.J. Pierson.** (1966). *Principles of Physical Oceanography*, Prentice-Hall, Inc., 506 pp.
- Oberhettinger, F. and L. Badii.** (1973). *Tables of Laplace Transforms*.
- Pond, S. and G.L. Pickard.** (1983). *Introductory Dynamical Oceanography*, 2nd edition, Pergamon Press, 329 pp.

This page intentionally left blank.

A Appendix

The linearized equation of motion for a pure drift current is given by Ekman (1905) as:

$$\frac{\partial w}{\partial t} + ifw = \nu \frac{\partial^2 w}{\partial z^2} \quad (15)$$

where $w = u + iv$ is the complex current of which u is the eastward velocity and v is the northward velocity. The Coriolis parameter is given by, $f = 2\Omega \sin \phi$ where Ω is the earth's rotation rate and ϕ is the latitude. The kinematic eddy viscosity is represented by ν and z is the vertical coordinate, positive upward.

The initial conditions are at rest:

$$w(z, 0) = \left. \frac{\partial w}{\partial t} \right|_{t=0} = 0, \quad (16)$$

and boundary conditions are no slip at the ocean bed:

$$w(-H, t) = 0 \quad (17)$$

where the water depth is given by H , and the wind stress at the ocean surface, F , is a function of time:

$$\nu \left. \frac{\partial w}{\partial z} \right|_{z=0} = F(t). \quad (18)$$

The method of solution to Equation 15 for an arbitrary and unsteady wind follows that given by Jelesnianski (1970). Equation 15 can be solved using a Laplace transform, such that:

$$s\hat{w}(z, s) = -if\hat{w}(z, s) + \nu \frac{\partial^2 \hat{w}(z, s)}{\partial z^2} \quad (19)$$

with boundary conditions

$$\hat{w}(-H, s) = 0, \quad \nu \left. \frac{\partial \hat{w}(z, s)}{\partial z} \right|_{z=0} = \hat{F}(s). \quad (20)$$

Again, following Jelesnianski (1970), assume the surface stress is an instantaneously applied constant force iF_0 with the resulting current, w_0 . Then, Equation 19 can be solved

$$\hat{w}_0 = \frac{iF_0 \sinh \alpha(H + z)}{\nu \alpha \cosh H\alpha} \quad (21)$$

where

$$\alpha = \sqrt{\frac{if + s}{\nu}}. \quad (22)$$

Equation 21 is solved using the inverse Laplacian and applying the s-shift property;

$$L^{-1}(\hat{f}(s + a)) = e^{-at} L^{-1}(\hat{f}(s)) = e^{-at} f(t). \quad (23)$$

The inverse Laplacian can then be found as

$$w_o = \frac{2iF_o}{H} \sum_{n=0}^{\infty} (-1)^n \sin \left[\left(n + \frac{1}{2} \right) (H + z) \frac{\pi}{H} \right] \exp \left[- \left\{ \left(n + \frac{1}{2} \right)^2 \frac{\nu \pi^2}{H^2} + if \right\} t \right]. \quad (24)$$

(see for instance, Oberhettinger and Badii, 1973).

If the restriction of a constant wind stress is replaced with a temporally varying wind, initially at rest, the solution to Equation 19 can then be given by

$$\hat{w}(z, s) = \frac{\hat{F}(s) \sinh \alpha(H + z)}{\nu \alpha \cosh H \alpha} = \frac{\hat{F}(s) \hat{w}_o}{iF_o}. \quad (25)$$

Solving, using Laplace convolution,

$$w = \frac{1}{iF_o} \int_0^t F(t - \tau) w_o d\tau. \quad (26)$$

Inserting Equation 24 into Equation 26, the wind drift current can be found from

$$w(z, t) = \frac{2}{H} \sum_{n=0}^{\infty} \cos \left[\left(n + \frac{1}{2} \right) \pi \frac{z}{H} \right] \int_0^t F(t - \tau) e^{-\theta_n \tau} d\tau \quad (27)$$

where θ_n is given by

$$\theta_n = if + \left[n + \frac{1}{2} \right]^2 \frac{\nu \pi^2}{H^2}. \quad (28)$$